# RSC Advances

ROYAL SOCIETY
OF CHEMISTRY

www.rsc.org/advances

1    **Anti-microbial efficiency of nano silver-silica modified geopolymer mortar for**

2    **eco-friendly green construction technology**

3    Dibyendu Adak[a], Manas Sarkar[b], Moumita Maiti[b], Abiral Tamang[b],

4    Saroj Mandal[a*] and Brajadulal Chattopadhyay[b]

5

6

7

8    [a] Department of Civil Engineering, Jadavpur University, Kolkata – 700032, India.

9    [b] Department of Physics, Jadavpur University, Kolkata – 700032, India.

10

11

12

13

14

15

16

17

18

19    • Corresponding author
20    Prof. Saroj Mandal
21    Phone: +91-9432236510
22    E. Mail: -mailtosarojmandal@rediffmail.com / smandal@civil.jdvu.ac.in
23

24    **Abstract:**

25    A silver-silica nano composite based geopolymer mortar has been developed by

26    simple adsorption of silver in a suitable amount of colloidal silica suspension for anti-

27    bacterial property development. The silver nanoparticles (3-7 nm) were attached on the

28    surface of 20-50 nm sized silica nanoparticle. The silver-silica nano-composite was

29    characterized by Transmission Electron Microscope (TEM), X-Ray Diffraction (XRD) and

30    Energy Dispersive X-ray Spectral analysis. Mechanical strength, durability and mechanistic

31    anti-bacterial activity of the silver-silica nano composite modified geopolymer mortar

32    ($GM_{Ag-Si}$) were investigated and compared to nano silica modified geopolymer mortar ($GM_{Si}$)

33    and control cement mortar (CM). To accesses the anti-microbial efficacy of the samples, 99%

34    mortality for the Gram positive and Gram negative bacteria were calculated. Minimum

35    Inhibitory Concentration (MIC) and Minimum Bactericidal Concentration (MBC) values

36    were determined from batch culture. With the addition of 6% (w/w) of silver-silica nano

37    composite in the geopolymer mortar cured at ambient temperature shows substantial

38    improvement in mechanical strength, durability and anti-bacterial property.  Reactive Oxygen

39    Species (ROS) generation and cell wall rapture as observed from fluorescence microscopy

40    and Field Emission Scanning Electron Microscopy (FESEM) may be possible reason behind

41    the anti-bacterial efficacy of silver-silica nano composite modified geopolymer mortar.

42

43

44

45    **Key Words:** Geopolymer, Silver-silica nano composite, Anti-bacterial, Mechanical Strength,

46    Durability.

## 1. Introduction:

The sustainability of the cement and concrete industries is imperative to the wellbeing of our planet and human development. The production of Portland cement, an essential constituent of concrete, releases greenhouse gas emissions both directly and indirectly. It is well accepted that about one tone of carbon dioxide ($CO_2$) is emitted into the atmosphere during the production of one tone of cement.[1] Coal based thermal power stations which produces a huge amount of fly ash which is annually estimated to be around 780 million tons throughout the world.[2] The utilization of fly ash is about 35% in construction of landfills, embankments, production blended cement etc. and remaining as an industrial hazards. Alkali activated geopolymer concrete/mortar have been introduced to reduce the rapid utilization of Portland cement concrete throughout the world. In the last few decades the application of geopolymer concrete using mainly fly ash (without cement) has becomes an important area of research.[3-6]

Geo-polymeric reaction generally depends on the activation with alkali solutions and temperature curing at 40–75 $^o$C to obtain similar strength and durability to normal concrete.[7-11] Thus the use of geopolymer concrete is limited to the precast member due to requirement of heat activation after casting. Several researchers have proposed to improve the strength development of fly ash based geopolymer cured at ambient temperature.[12-14] Geopolymer mortar, with the addition of 6% nano silica shows appreciable improvement in mechanical strength and durability at 28 days under ambient temperature curing.[15] However, it is necessary to explore the role of geopolymer composite different aspects like structural behavior and in the application of antimicrobial field.

Usually fresh concrete/mortar has a pH of 10 to 12 depending upon the mixture. Consequently with this high alkalinity it does not allow the growth of any microbes.

71    However, this high pH is slowly reduced over the time due to presence of carbon dioxide

72    ($CO_2$) and hydrogen sulfide ($H_2S$) in the atmosphere producing week acids (carbonic acid,

73    thio-sulphuric acid etc.) in presence of water. When pH of the concrete/ mortar is reduce to

74    below 9.0, bacterial attack or deposition on concrete surface begins.[16] The microbial colonies

75    on the concrete surface, capillaries and micro/macro fissures cause concrete damage through

76    bio-deterioration.[17] Bio-deterioration of conventional concrete structure such as sewage pipes,

77    maritime structures, bridges, tanks, pipelines and cooling towers occurs due to the presence of

78    harmful bacteria.[18&19] Various studies suggest that use of silver NPs in minimum

79    concentration shows promising anti-bacterial property.[20&21] With this background, use of

80    silver-silica nano composite modified low calcium based fly-ash geopolymer mortar cured at

81    ambient temperature, may be a favorable contender to Portland cement concrete. In this

82    study, mechanical strength, durability and mechanistic anti-bacterial activity of fly ash based

83    silver-silica nano composite modified geopolymer mortar ($GM_{Ag-Si}$) has been investigated and

84    compared with silica modified geopolymer mortar ($GM_{Si}$) and control cement mortar (CM).

85    **2. Materials and method**:

86    **2.1 Ingredients:**

87        Low Calcium Class F dry fly ash, locally available sand (Specific gravity 2.52, water

88    absorption 0.50%, and fineness modulus of 2.38), alkali activator fluid (mixture of sodium

89    hydroxide, sodium silicate and deionized water) have been used as basic ingredients of

90    geopolymer mortar.[22&23] For control cement mortar, Ordinary Portland Cement (OPC) and

91    deionized water has been used.

92        Nutrient Broth (NB) media ingredients like peptone, beaf extract, Yeast extract,

93    NaCl, agar (Hi-media Pvt. Ltd., India), silver nitrate (Merck Germany), deionized water,

94    carbonic acid, *E. coli* (MTCC 1652 strain), *S. aureus* (MTCC 96 strain) bacteria have been

95    used. All reagents were prepared with milli-Q ultra-pure water. The basic properties of

96    colloidal nano silica, as provided by the manufacturer, are mentioned in Table-1.

**2.2 Preparation of silver silica nano composite:**

98    For preparation of silver nanoparticles (Ag NPs) on the surface of colloidal silica

99    nanoparticles ($SiO_2$ NPs), 100 mM colloidal silica NPs water solution was taken and the 5

100   mM silver nitrate ($AgNO_3$) were added drop-wise under vigorous stirring at ambient

101   temperature for 6h.[24]

**2.3. Confirmative test for silver-silica nano composite**

103   The silver-silica nano solution was lyophilized (EYELA FDU-1200, Japan) and

104   crushed to make a uniform fine powder. The surface morphology of the synthesized nano

105   structured samples were evaluated using High Resolution Transmission Electron Microscopy

106   (HRTEM; JEOL, JEM 2100). The surface charges and size distribution of silica NPs and

107   silver-silica nano composite were determined by using Zeta Potential Analyzer (Brookhaven

108   Instruments Corp. Holtsville, USA). XRD analysis was performed (Bruker AXS, Inc., Model

109   D8, WI, USA) with mono-chromatised Cu-Kα radiation of wavelength 1.5406 Å at 55 kV and

110   40 mA. The sample was examined at 2θ from $10^o$ to $80^o$ and identified by referring to data of

111   Joint Committee on Powder Diffraction Standards (JCPDS) files.

**2.4. Preparation of mortar mixtures ($GM_{Si}$, $GM_{Ag-Si}$ and CM):**

113   Two different fly-ash based geopolymer mortars ($GM_{Si}$, $GM_{Ag-Si}$) and a conventional

114   control mortar (CM) were prepared for the present study. The activator fluid to fly ash ratio

115   was taken at 0.40. The activator fluid was made by mixing 12M NaOH with $Na_2SiO_3$ at

116   weight ratio of 1:1.75. This solution was mixed with colloidal nano silica solution

117   (activator 1) for the preparation of $GM_{Si}$ geopolymer specimens. For preparation of $GM_{Ag-Si}$

118    geopolymer mortar, activator 2 was prepared by 12M NaOH and $Na_2SiO_3$ at same weight

119    ratio with nano silver-silica solution. The amount of nano silica and silver-silica nano

120    composite in the respective activator 1 and activator 2 solutions was 6% (w/w) of fly ash

121    used. For the preparation of control mortar sample (CM), OPC of 43 grade sand and distilled

122    water were used.[25] Details of all mixes are shown in Table 2. For determination of mechanical

123    strength (compressive strength, flexural and split tensile strength) and durability (RCPT), the

124    samples of mix $GM_{Si}$ and $GM_{Ag-Si}$ were removed from the mould after 24 h and kept in

125    ambient temperature and tested after 3, 7 and 28 days of air curing. Conventional water

126    curing was made for the CM specimens until the test.

127    **2.5. Sample preparation and testing of mechanical strength:**

128          The standard mortar cube specimens of dimension 70.6 mm × 70.6 mm × 70.6 mm

129    were prepared for different mixes to determine the compressive strength of mortars. All the

130    specimens were tested at 3 days, 7 days, and 28 days after casting to determine the

131    compressive strength. Flexural strength testing was carried out on mortar bars (50 mm × 50

132    mm × 200 mm) for all ($GM_{Si}$, $GM_{Ag-Si}$, CM) samples. The center point loading method was

133    adopted for the determination of flexural strength (ASTM C293).[26] Cylinder specimens (100

134    mm diameter × 200 mm height) were tested for split tensile strength test for each category

135    after 28 days from the date of casting.

136    **2.6. Durability test:**

137          Rapid Chloride ion Penetration Test (RCPT) was adopted for the durability

138    assessment of different mortar mixes. Test cylinder specimens (100 mm diameter × 200 mm

139    height) were sliced into core specimens of thickness 50 mm and subjected to RCPT by

140    impressing 60V.[27] All the specimens were tested after 28 days of casting.

141

142　**2.7. Anti-bacterial Study:**

143　　　　　Mortar samples ($GM_{Si}$ and $GM_{Ag-Si}$ & CM) were immersed in 0.5 N Carbonic acid

144　solutions until the pH value of all samples become less than 9.0. After getting the pH<9.0, the

145　samples were crushed by hand mortar and sieved in uniform sized powder for the anti-

146　bacterial study purpose.

147　**2.7.1. Bacterial kinetics study:**

148　　　　　Bacterial kinetics of mortar samples from $GM_{Si}$, $GM_{Ag-Si}$ and CM were investigated

149　against *S. aureus* (gm +ve) and *E. coli* (gm −ve) bacterial strains distinctly. From an overnight

150　growing fresh culture of both bacteria, a volume of culture approximately representing ~$10^7$

151　CFU/ml was washed and suspended in PBS buffer. The fresh culture was then diluted by 5 ml

152　nutrient broth (0.5% peptone, 0.1% beef extract, 0.2%Yeast extract, 0.5% NaCl, pH 7) at a

153　final cell concentration of $10^4$ CFU/ml and incubated at 37 $^o$C. For anti-bacterial assay, 2

154　mg/ml (~2 × MIC) of each dry dust samples (pH < 9) ($GM_{Si}$, $GM_{Ag-Si}$ and CM) were used to

155　treat the inoculated broth separately. Time dependent killing was determined by plating the

156　culture from the treated geopolymer mortar samples and control cement mortar sample in

157　agar plate (15%) after different time of incubation (0, 2, 4, 6, 8, 12, 24 h). Plates were

158　incubated at 37 °C and the numbers of colonies were counted after 24 h. The whole

159　experiment was repeated trice.

160　**2.7.2. Determination of MIC and MBC test:**

161　　　　　Using batch culture process, the Minimum Inhibitory Concentration (MIC) was

162　observed by the varying concentration of different geopolymer samples.[28] Growth medium

163　containing initial cell concentration ($10^7$ CFU/ml) of each strain was taken distinctly. The

164　different mortar powders ($GM_{Si}$, $GM_{Ag-Si}$ and CM) were added in the growth medium

165 distinctly and inoculated at 37 $^{\circ}$C on a rotary shaker. In 5ml NB, the powder samples (0.1% -

166 5.0 % w/v) of each category were added separately in several marked tubes. The growth

167 inhibitions (GM$_{Si}$ and GM$_{Ag-Si}$ treated bacterial cells) were measured against control at 620

168 nm by a UV-visible Spectrophotometer (ELICO, SL 196 Spectropharm).[29&30]

169        Minimum bactericidal concentration (MBC) is defined as the lowest concentration of

170 silver nanoparticles present in GM$_{Ag-Si}$ samples that kills 99.9% of the bacteria. The presences

171 of viable microorganisms were examined and lowest concentrations causing bactericidal

172 effect were reported as MBC for the growth inhibitory concentrations.[31] The experiment was

173 performed by plating (Nutrient Agar plate 15%) the bacterial cultures with upper amounts

174 above the MIC. The agar plates were inoculated at 37 $^{\circ}$C for 24 h. All the experiments were

175 carried out in triplicate.

176 **2.7.3. Reactive oxygen species (ROS) detection and fluorescence microscopic analysis:**

177        The generations of superoxide radical activity were measured according to method

178 given by Su et al.[32] freshly prepared pure log phased cultures of *E. coli* and *S. aureus* were

179 taken separately for this purpose. $10^4$ CFU/ml containing fresh NB were inoculated and

180 treated with GM$_{Si}$ and GM$_{Ag-Si}$ with their MIC values at 37 °C for 1h distinctly. Bacterial

181 pellets were washed with Phosphate buffer (pH 7.0) several times and treated with 10 μM

182 DCFHDA for 30 min. So that DCFDA diffuses through the cell membrane, enzymatically

183 hydrolyzes by intracellular esterase and oxidizes to produce a fluorescent 2′, 7′-

184 dichlorofluorescein (DCF) in the presence of ROS. From fluorescence spectrophotometer, the

185 ROS level was measured at 490 nm (excitation) and emission at 520 nm using SYBR Green

186 and PI for living and dead cells respectively. The intensity of fluorescence is proportional to

187 the level of intracellular reactive oxygen species.[33] The working solution of 10 μl each of

188 SYBR Green DMSO solution (1:100 v/v) and PI water solution (1mg/ml) were taken in to 1

189    ml of each treated $GM_{Si}$ & $GM_{Ag-Si}$ and CM samples. After incubation at 37 $^{o}$C for 30 min,

190    each sample was mounted immediately over slides and pictures were captured by the

191    fluorescence microscope for this experiment.[34]

192    **2.7.4. Morphological investigation for bacterial strains:**

193        Certain volume of NB medium and powder samples of the three different mortar

194    specimens ($GM_{Si}$, $GM_{Ag-Si}$ & CM) were added separately to 5 ml cultures of each bacteria

195    resulting in final concentration of 1mg/ml samples and bacterial concentration of $10^{8}$

196    CFU/ml. This experiment was performed for both bacteria (*E. coli* & *B. subtilis*) and for three

197    different test samples separately. For morphological analysis, bacterial growth medium in mid

198    exponential phase and with the same cell density were treated with samples ($GM_{Si}$, $GM_{Ag-Si}$

199    and CM) for 6h at 37 °C. The bacterial samples were then washed with milli-Q water, fixed

200    with 2% glutaraldehyde and placed on a silicon platelet (Plano, Wetzlar, Germany). A series

201    of ethanol dehydration steps were carried out followed by staining with 3% uranyl acetate in

202    25% ethanol. Finally, the samples were washed with buffer solution (0.1 M sodium

203    phosphate, pH 7.2) and investigated using FESEM (INSPECT F50 SEM, The Netherlands).

204    **2.7.5. DNA agarose gel electrophoresis:**

205        The genomic DNA were isolated from the cells (*E. coli* & *S. aureus*) and purified by

206    phenol chloroform method. 1μl of $GM_{Si}$ and $GM_{Ag-Si}$ water solution (1μg/ml) were mixed to

207    the extremely pure two types of naked DNA separately. After 15 min incubation at room

208    temperature, the treated and pure DNA was run in 1% low melting agarose gel. The images of

209    DNA were taken under trans-illuminator (Fotodyne 110-V UV Trans-illuminator).

210

211

212     **Statistical analysis:**

213            Experiments were performed in triplicate. Error bars on graph represent the standard

214     error.  One way ANOVA was used to compare three or more groups defined by a single

215     factor. Comparisons were made between two different geopolymer samples ($GM_{Si}$ and

216     $GM_{Ag-Si}$) and control samples (CM) with the treatment of two types of different microbial

217     strains. All data were expressed as mean ± SD of six separate experiments. Where N ≥ 10

218     were taken for each category.

219

220     **3. Results:**

221     **3.1. Characterization of nano silver silica composite:**

222            Transmission Electron Microscopy analysis of silica NPs and silver-silica nano

223     composite shows their very regular spherical shape (fig. 1A & 1B). Figure 1B shows the

224     silver NPs (mean ± SD: 4 ± 1 nm) are formed on the surface of silica NPs (30 ± 10 nm).

225     Elemental analysis of newly synthesized silica NPs and silver-silica nano composites are

226     shown in figure 1A & 1B (inset).  The presence of the elements O and Si were observed at

227     0.562 KeV (O), 1.75 KeV (Si) respectively. The Si, O and Ag peaks are clearly shown in

228     figure 1B (inset), which indicates that the presence of silver nano particles on to the silica

229     surface. It was confirmed from TEM images that nano-particles are pure in colloidal form but

230     the particles are of hybrid-type in silver-silica nano composites. Also the average size of the

231     silica NPs 20-40 nm was analyzed by using Zeta size distribution graph (fig. 1 C-I). The

232     silver NPs (4 ± 1 nm) were attached on the surface of silica NPs which was showed in figure

233     1D-I. Also in figure 1D-I, comparatively broad peak is revealed that the greater size

234     distribution of silver-silica nano composite, which is also much correlated with TEM result

235     (fig. 1B). The overall surface charge of the pure silica NPs (fig. 1C-II) was negative (-50 mV)

236     whereas silver silica nano-composite (fig. 1D-II) showed some greater positive charges (>-50

237     mV) which was confirmed by zeta potential analysis.

238         The X-ray Diffraction profiles of newly synthesized silica NPs and silver-silica nano-

239     composite were matched up with JCPDs data file (fig. 2A). The XRD pattern of silver-silica

240     NPs showed the presence of sharp peaks which are absent in silica NPs. The sharp peaks

241     indicate that the newly synthesized nano particles are either very small crystallite size or

242     semi-crystalline in nature. The average crystallite size of silver nano particles were estimated

243     by Scherrer's equation for the (122), (220), and (222) diffraction peaks at $2\theta$=38.118, 45.593,

244     57.937 and 71.101 respectively. Therefore, it is clearly confirmed that silver-silica nano

245     composite particles were successfully synthesized.

246     **3.2 Presence of silver NPs in GM$_{Ag-Si}$ mortar:**

247         The XRD spectra of nano silica modified geopolymer mortar (GM$_{Si}$) and nano silver-

248     silica nano composite modified geopolymer (GM$_{Ag-Si}$) mortar were represented in figure 2B.

249     In case of geopolymer mortar with nano silver-silica composite, some additional peak

250     positions were observed at same specific positions ($2\theta$) that confirmed the presence of silver

251     nano particles in GM$_{Ag-Si}$ mortar.

252     **3.3. Strength and durability of different mortars:**

253         Figure 3A represents the compressive strength of fly ash based nano silica modified

254     geopolymer (GM$_{Si}$) mortar and nano silver-silica modified geopolymer mortar (GM$_{Ag-Si}$)

255     samples cured at ambient temperature. The strength of control sample made from OPC

256     cement was also compared. It was observed that both the geopolymer mortar samples (GM$_{Si}$

257     and GM$_{Ag-Si}$) show better compressive strength than CM samples at all ages. However,

258     addition of silica NPs and silver-silica nano composite (6% of fly ash by weight) in

259     geopolymer mortar seems to provide similar compressive strength cured at ambient

260     temperature. It is noted that the presence of silver NPs attached on the surface of silica NPs

261   do not affect the strength of modified geopolymer mortar.[15] Similar behavior was also

262   observed on flexural strength and split tensile strength of geopolymer mortars and control

263   mortar samples (fig. 3B). A comparison of RCPT value for $GM_{Si}$, $GM_{Ag-Si}$ and CM samples

264   were presented in figure 3C. It is observed that less amount of ions passed through

265   geopolymer ($GM_{Ag-Si}$ and $GM_{Si}$) matrices than CM matrices. This indicates that the diffusion

266   coefficient will be less due to presence of crystalline compound in $GM_{Si}$ and $GM_{Ag-Si}$

267   modified geopolymer mortars thereby improving the durability.

268   **3.4. Anti-bacterial study:**

269        The bactericidal kinetics of exponentially growing gram negative *E. coli* and gram

270   positive *S. aureus* bacteria were observed against $GM_{Si}$, $GM_{Ag-Si}$, and CM samples by time

271   killing assay. The result revealed that the populations of *E. coli* and *S. aureus* bacteria were

272   reduced by 99% after 8h and 6h (fig. 4C & 4D) for $GM_{Ag-Si}$ respectively. The anti-bacterial

273   effect was shown by plate culture of bacteria after 8h treatment (fig. 4A & 4B). A large

274   number of colonies were found in $GM_{Si}$ and control specimens whereas none was seen in case

275   of $GM_{Ag-Si}$ sample.

276        The MIC and MBC values of $GM_{Ag-Si}$ sample against gram +ve and gram-ve

277   microorganisms are represented in Tables 3 and 4. Table 3 indicates that considerably low

278   amount of $GM_{Ag-Si}$ (0.15 mg/mL) was able to eradicate the gram (–ve) bacterial cells (>99%).

279   Gram -ve organisms were more resistant to the growth inhibiting effect of the sample (0.10

280   mg/mL) compared to gram +ve bacterial cell. The anti-bacterial activities of $GM_{Ag-Si}$

281   geopolymer mortar samples are significantly higher than the other specimens ($GM_{Si}$ &

282   control sample). The MBC for silver-silica nano composite treated cells are not more than 4

283   times their respective MIC values indicating that the nano composites are bactericidal rather

284   than bacteriostatic. The MBC value (Table 4) indicates that considerably lower amount of

285    silver (0.43 µg/ml) was able to eradicate the gram positive bacterial (*S. aureus*) cells. The

286    gram negative organisms (*E. coli*) were more resistant to the growth inhibiting effect of silver

287    NPs (0.32 µg/ml).

288         The ROS level of the cells (*E. coli* & *S. aureus*) treated with $GM_{Si}$ and $GM_{Ag-Si}$ were

289    compared to CM treated cells. The level of ROS for the CM treated cells was considered as

290    100%. For $GM_{Ag-Si}$ treated cells the intensity was about 5 times higher with respect to the

291    control for both *E. coli* and *S. aureus* (fig. 5A). As observed, the oxidative stress in the

292    $GM_{Ag-Si}$ treated cells was much higher as compared to the CM and $GM_{Si}$ treated micro-

293    organisms.

294         The purified bacterial genomic DNA of *E. coli* and *S. aureus* are shown (fig. 5B) in

295    Gel electrophoresis (lane-1 and lane 4) whereas the $GM_{Si}$ treated DNA was observed in lane-

296    2 and lane-5. The $GM_{Ag-Si}$ treated DNA was fragmented in lane -3, lane-6.

297         The SYBR Green is a bacterial cell membrane permeant dye which stains both live

298    and dead cells. The fluorescence microscopic images show that control cells and $GM_{Si}$ treated

299    cells (*E. coli* and *S. aureus*) are intensely stained with SYBR Green whereas $GM_{Ag-Si}$ treated

300    cells are found to be PI positive (fig. 6). The PI is an impermeant dye that stains only dead

301    and membrane compromised cells due to loss of the plasma membrane integrity. The result of

302    morphological analysis of $GM_{Ag-Si}$ treated cells represents extensive membrane destruction

303    and disruption of cells after 8h of incubation (fig. 7C) in respect to control and $GM_{Si}$ treated

304    *E. coli* cells (fig 7A and 7B) respectively. Control and $GM_{Si}$ treated cells shows distinct

305    spherical morphology of coccus shaped *S. aureus* (fig. 7D and 7E respectively), whereas

306    membrane deformation and pore formation can be seen along with cell debris in case of

307    $GM_{Ag-Si}$ treated cells (fig. 7F).

308

309   **4. Discussion:**

310        In this present study, the silver NPs (2-5 nm) has been attached on the surface of silica

311   NPs of 30-50 nm (Fig. 1B) to develop the antimicrobial activity of the geopolymer mortar. In

312   presence of positively charged silver NPs on the surface of the negatively charged silica NPs,

313   the overall charges of silver-silica nanocomposite (fig. 1C-II) is reduced. The incorporation of

314   this newly formed silver NPs in the low calcium fly-ash based geopolymer mortar has

315   improved its anti-bacterial property. However, the strength and durability do not affected due

316   to the presence of such silver NPs in geopolymer mortar cured at ambient temperature. The

317   strength and durability of geopolymer mortar ($GM_{Ag-Si}$) is not affected by the presence of

318   silver NPs (fig. 3). The silver has the potential to kill bacteria in minimum time period.[29&35]

319   The different bacterial cell wall disruptions (fig. 7) indicate that the anti-bacterial property

320   has been developed in desired geopolymer mortar. Silver-silica nano composite having 6% by

321   weight of fly ash in geopolymer mortar was sufficient to resist the bacterial growth. The

322   growth for both types of bacteria (gram –ve / gram + ve) was stopped within 6-8h only in

323   presence of silver NPs modified $GM_{Ag-Si}$ geopolymer mortar. Bacterial growth population in

324   general depends on numerous external factors like pH, temperature, concentration of nano-

325   particles.[36&37] In various studies, it is reported that due to the high alkali property of fresh

326   concrete/mortar at early age, it will not allow any bacterial growth. However, the pH of

327   concrete / mortar is slowly reduced over time by the effect of carbon dioxide and hydrogen

328   sulfide gas and growth of bacteria starts.

329        Silver silica nano composite modified geopolymer mortar shows better resistance to

330   bacterial attack than nano silica modified geopolymer and control samples. Silver nano

331   particles incapacitate enzymes through binding of sulfhydryl (thiol) groups in amino acids of

332   bacterial cell and promote the release of ions/NPs with subsequent hydroxyl radical

333   formation.[38&39] Gram-negative bacteria possess an outer membrane outside the peptidoglycan

334    layer which is absent in Gram-positive organisms.[40] The outer membrane protects bacteria

335    from harmful agents, such as detergents, drugs, toxins and degradative enzymes by

336    functioning as selective permeability barrier. The cell wall disruption by the lower amount of

337    silver NPs in geopolymer particle (~MIC) may be the main reason of bactericidal kinetics.

338    Farther, the unfavorable intracellular ROS generation also facilitates to destroy these bacteria

339    by biological targeting of DNA, RNA, proteins and lipids. Initiation of lipid peroxidation via

340    damage of membrane Poly unsaturated fatty acids was caused by free radical generation.

341    The effect of silver NPs on bacteria is observed by the structural and morphological

342    changes (fig. 7). It is suggested that in undisturbed state, the replication of DNA can be

343    effectively conducted and loses its replication ability in that form. The DNA molecule turns

344    into condensed form and loses its replication ability when the presence of silver ions/NPs

345    within the bacterial cell, leading to cell death.[41] The DNA damage images (fig. 5B) are also

346    correlated with the previously reported discussion.

347    The influence of lipid peroxidation process shrinks the membrane fluidity through

348    alteration membrane properties and can disrupt membrane-bound proteins significantly.[42] In

349    contact of silver NPs, DNA was completely destroyed and fragmented (fig. 5B). The activity

350    of the silver NPs was extremely detrimental for DNA molecules by breaking its double

351    helical structure. DNA loses its replication ability and cellular proteins become inactivated on

352    silver NPs treatment.[41]

353    **5.0 Conclusion:**

354    It may be concluded that low calcium fly ash based silica modified geopolymer

355    mortar cured at room temperature shows almost similar strength and durability but better anti-

356    bacterial property. Silver-silica modified geopolymer mortar demonstrates better anti-

357    bacterial property than conventional cement mortar and silica modified geopolymer mortar.

358    Due to positive charge, silver NPs in the liquid growth medium are attracted electrostatically

359    to the negatively charged cell wall of bacteria. A few oxidized silver ions/NPs also get

360    attached electrostatically to the bacterial membrane and thus decreases the osmotic stability

361    of the cell, trailed by consequent leakage of intracellular constituents. The anti-bacterial

362    activity of $GM_{Ag-Si}$ was developed by introducing silver NPs on the surface of silica NPs

363    which is the main ingredients for anti-bacterial activity of geopolymer mortar. It is an

364    ecofriendly, non-hazard, cost effective and more durable building materials which can show

365    the new hope for better green construction technology.

366

367

368

369

370

371

372

373

374

375

376

377

378

**5. Reference:**

1.  P. K. Mehta, *Concrete International,* October 2001, 23(10):61–6.

2.  World of Coal Ash (WOCA) conference; Lexington; April 22-25, 2013;

3.  J. Davidovits, *Journal of Thermal Analysis*, 1991, 37, 1633–56.

4.  D. Hardjito, S. E. Wallah, V. Rangan, and B. V. Rangan, *Australian Journal of Structural Engineering*, 2005, 6, 1-9.

5.  J. A. Fernandez, M. Monzo, M. V. Cabedo, A. Barba and A. Palamo, *Microporous Mesoporous Materials*, 2008, 108,41–9.

6.  Z. Xie, Y. Xi, *Cement Concrete Research*, 2001, 31, 1245–1249.

7.  P. Chindaprasirt, T. Chareerat, V. Sirivivatnanon, *Cement Concrete Composites*, 2007, 29, 224–229.

8.  S. Pangdaeng, T. Phoo-ngernkham, V. Sata and P. Chindaprasirt, *Material & Design*, 2014, 53, 269–274.

9.  M. S. Villarreal, A. M. Ramíreza, S.S. Bulbarelaa, J. R. Gasca-Tirado, J. L. Reyes-Araiza and J. C. Rubio-Avalos, *Materials Letters*, 2011, 65, 995–998.

10. G. Gorhan, G. Kurklu, *Composites Part B: Engineering*, 2014, 58 371-377.

11. F. F. V. Barbosa, J. D. K. Mackenzie, C. Thaumaturgo, *International Journal of Inorganic Materials*, 2000, 309-317.

12. J. Temuujin, R. P. Williams, A. Van. Riessen, *Journal of Materials Processing Technology*, 2009, 209, 5276–5280.

13. P.S. Deb, P. Nath, P. K. Sarkar, *Advance Material Research*, 2013, 05, 168-173.

14. H. M. Giasuddin, G. Sanjayan, P.G. Ranjith, *Fuel*, 2013, 07, 34-39.

15. D. Adak, M. Sarkar, S. Mandal, *Construction and Building Materials*, 2014, 70, 453-459.

16. Con Shield: Technical presentation; Orlando, Florida, 1998.

404    17. H. Viitanen, J. Vinha, K. Salminen, *Journal of Building Physics*, 2010, 33, 201-224.

405    18. A. K. Parande, P. L. Ramsamy, S. Ethirajan, C. R. K. Rao and N. Palanisamy,

406       *Proceedings of the ICE - Municipal Engineer*, 2006, 159, 11-20.

407    19. M. Sanchez-Silva, D. Rosowsky, *Journal of Materials in Civil Engineering*. 2008, 20,

408       352–365.

409    20. A. Panáček, L. Kvítek, R. Prucek, M. Kolář, R. Večeřová, N. Pizúrová, V. K. Sharma,

410       T. Nevěčná, and R. Zbořil, *Journal of Physical Chemistry B*, 2006, 110, 16248–

411       16253.

412    21. J. R. Morones, J. L. Elechiguerra, A. Camacho, K. Holt, J. B. Kouri, J. T. Ramírez,

413       and M. J. Yacaman, *Nanotechnology*, 2005, 16, 2346-2353.

414    22. ASTM C618-12a: Standard Specification for Coal Fly Ash and Raw or Calcined

415       Natural Pozzolan for Use in Concrete; ASTM International, West Conshohocken, PA,

416       2012.

417    23. D. Adak, S. Mandal, *Indian Concrete Journal*, 2015, 89, 31-40.

418    24. V. Pol, D. N. Srivastava, O. Palchik, V. Palchik, M. A. Slifkin and A. M. Weiss,

419       *Langmuir*, 2002, 18, 3352–3357.

420    25. M. Sarkar, T. Chowdhury, B. Chattopadhyay, R. Gachhui and S. Mandal, *Journal of

421       Materials Science*, 2014, 49, 4461-4468.

422    26. ASTM C293-10: Standard Test Method for Flexural Strength of Concrete (Using

423       Simple Beam with Center-Point Loading); ASTM International, West Conshohocken,

424       PA, 2010.

425    27. ASTM C1202-12: Standard Test Method for Electrical Indication of Concrete's

426       Ability to Resist Chloride Ion Penetration; ASTM International, West Conshohocken,

427       PA, 2012.

428    28. L. Qi, Z. Xu, X. Jiang, C. Hu and X. Zou, *Carbohydr Research*, 2004**,** 339, 2693–700.

429    29. J. Ruparelia, A. Chatterjee, S. P. Duttagupta and S. Mukherji, *Acta-Biomaterial*, 2008,

430        4, 707–716.

431    30. G. Ren, D. Hu, C. Cheng, M. A. Vargas-Reus, P. Reip, R. P. Allaker, *International*

432        *Journal of Antimicrobial Agents*, 2009, 33, 587-590.

433    31. M. R. Avadia, A. M. M. Sadeghib, A. Tahzibic, Kh. Bayati, M. Pouladzadeh, Z. Mehr

434        and M. R. Thehrani, *European Polymer Journal*, 2004, 40, 1355–1361.

435    32. H. L. Su, C. C. Chou, D. J. Hung, S. H. Lin, I. C. Pao, J. H. Lin, F. L. Huang,

436        R. X. Dong and J. J. Lin, *Biomaterials*, 2009, 30, 5979–5987.

437    33. S. A. Shoichet, A. T. Bäumer, D. Stamenkovic, H. Sauer, A. F. Pfeiffer, C. R. Kahn,

438        D. M. Wieland, C. Richter and M. Ristow, *Human Molecular Genetics*, 2002, 11,

439        815-821.

440    34. S. Barbesti, S. Citterio, M. Labra, M. D. Baroni, M. G. Neri and S. Sgorbati,

441        *Cytometry*, 2000, 40, 214–218.

442    35. S. Agnihotri, S. Mukherji, S. Mukherji, *RSC Advances*, 2014, 4, 3974-3983.

443    36. J. S. Kim, E. Kuk, K. N. Yu, *Nanomedicine*, 2007, 3, 95-101.

444    37. F. Rispoli, A. Angelov, D. Badia, A. Kumar, S. Seal and V. Shah, *Journal of*

445        *Hazardous Materials*, 2010, 180, 212–216.

446    38. M. R. Yeaman, N. Y. Yount, *Pharmacological Reviews*, 2003, 55, 27-55.

447    39. N. A. Amro, L. P. Kotra, K. W. Mesthrige, A. Bulychev, S. Mobashery and G. Liu,

448        *Langmuir*, 2000, 16, 2789–2796.

449    40. H. Nikaido, *Microbiol Mol Biol Rev*, 2003, 67, 593–656.

450    41. Q. L. Feng, J. Wu, G. Q. Chen, F. Z. Cui, T. N. Kim and J. O. Kim, *J Biomed Mater*

451        *Res*., 2000, 52, 662-668.

452    42. E. Cabiscol, J. Tamarit, J. Ros, *International Microbiology*, 2000, 1 3, 3-8.

453

454    **Table 1:** Basic Properties of Colloidal Nano silica:

| Colloidal Nano Silica type | Average particle size (nm) | Solid content (% Wt.) | Viscosity (Pa S) | pH | Solid density (g/cm$^3$) |
|---|---|---|---|---|---|
| CemSynXTX | 20 to 50 nm | 31% | 8.5 | 9.0 - 9.6 | 2.16 |

464    **Table 2:** Nano silica modified geopolymer (GM$_{Si}$), silver silica modified geopolymer mortar

465            (GM$_{Ag-Si}$) and control mortar (CM), mix proportions:

| Sample Mark | Fly ash: sand | Activator Solutions | % of SiO$_2$ NPs | % of Ag-SiO$_2$ NPs | Curing condition |
|---|---|---|---|---|---|
| GM$_{Si}$ | 1:3 | Activator-1 | 6.0 | Nil | Air curing at room temp. |
| GM$_{Ag-Si}$ | 1:3 | Activator-2 | Nil | 6.0 | Air curing at room temp. |
| CM (Cement: sand) | 1:3 | Water | Nil | Nil | Water curing. |

480    ** Activator -1 - NaOH+Na$_2$SiO$_3$+Nano Silica

481    ** Activator -2 - NaOH+Na$_2$SiO$_3$+Nano Silver-Silica

487 **Table: 3**

488 MIC ASSAY:

489

| Bacteria | Control (mg/ml) | $GM_{Si}$ (mg/ml) | $GM_{Ag-Si}$ (mg/ml) |
|----------|-----------------|-------------------|----------------------|
| *E. coli* | --- | --- | 0.10 |
| *S. aureus* | --- | --- | 0.15 |

494

495

496

497

498
499 **Table: 4**
500
501 MBC ASSAY:
502

| Bacteria | Control (mg/ml) | $GM_{Si}$ (mg/ml) | $GM_{Ag-Si}$ (mg/ml) |
|----------|-----------------|-------------------|----------------------|
| *E. coli* | --- | --- | 0.32 |
| *S. aureus* | --- | --- | 0.43 |

507

508

509

510

511

512

513    **Figure legends**

514    Figure 1: TEM image of (A) Silica NPs & (B) Silver-silica NPs with inset representing

515            elemental analysis by EDS. Zeta size (C-I & D-I) and Zeta potential (C-II & D-II)

516            distribution graph of silica NPs & silver-silica NPs respectively.


517    Figure 2A: XRD spectra of (I) $SiO_2$ NPs & (II) $Ag\text{-}SiO_2$ NPs.

518    Figure 2B: XRD spectra of (I) $GM_{Si}$ and (II) $GM_{Ag\text{-}Si}$.

519    Figure 3: (A) Compressive strengths, (B) flexural & tensile strengths, (C) RCPT of different

520            mortar samples (CM, $GM_{Si}$ & $GM_{Ag\text{-}Si}$).

521    Figure 4: Photographs of colonies of (A) *E. coli* & (B) *S. aureus* incubated on agar plates

522            obtained from cultivated suspensions with (CM, $GM_{Si}$ & $GM_{Ag\text{-}Si}$). Mortality

523            curve of (C) Gram –ve bacteria (D) Gram +ve bacteria in presence of CM, $GM_{Si}$

524            & $GM_{Ag\text{-}Si}$.

525    Figure 5: ROS count of (A) different samples and (B) Gel electrophoresis images

526            Lane-1: CM treated DNA (*E. coli*), Lane-2: $GM_{Si}$ treated DNA (*E. coli*),

527            Lane-3: $GM_{Ag\text{-}Si}$ treated (*E. coli*), Lane-4: CM treated DNA (*S. aureus*),

528            Lane-5: $GM_{Si}$ treated DNA (*S. aureus*), Lane-6: $GM_{Ag\text{-}Si}$ treated DNA (*S.*

529            *aureus*).


530    Figure 6: Fluorescence microscopic images of (A) CM treated *E. coli*, (B) $GM_{Si}$ treated *E.*

531            *coli*, (C) $GM_{Ag\text{-}Si}$ treated *E. coli*, (D) CM treated *S. aureus*, (E) $GM_{Si}$ treated *S.*

532            *aureus*, (F) $GM_{Ag\text{-}Si}$ treated *S. aureus* bacterial cells.


533    Figure 7: FESEM images of (A) CM treated *E. coli*, (B) $GM_{Si}$ treated *E. coli*, (C) $GM_{Ag\text{-}Si}$

534            treated *E. coli*, (D) CM treated S. *aureus*, (E) $GM_{Si}$ treated *S. aureus* and (F)

535            $GM_{Ag\text{-}Si}$ treated *S. aureus*.


536

1    **Figures:**

2
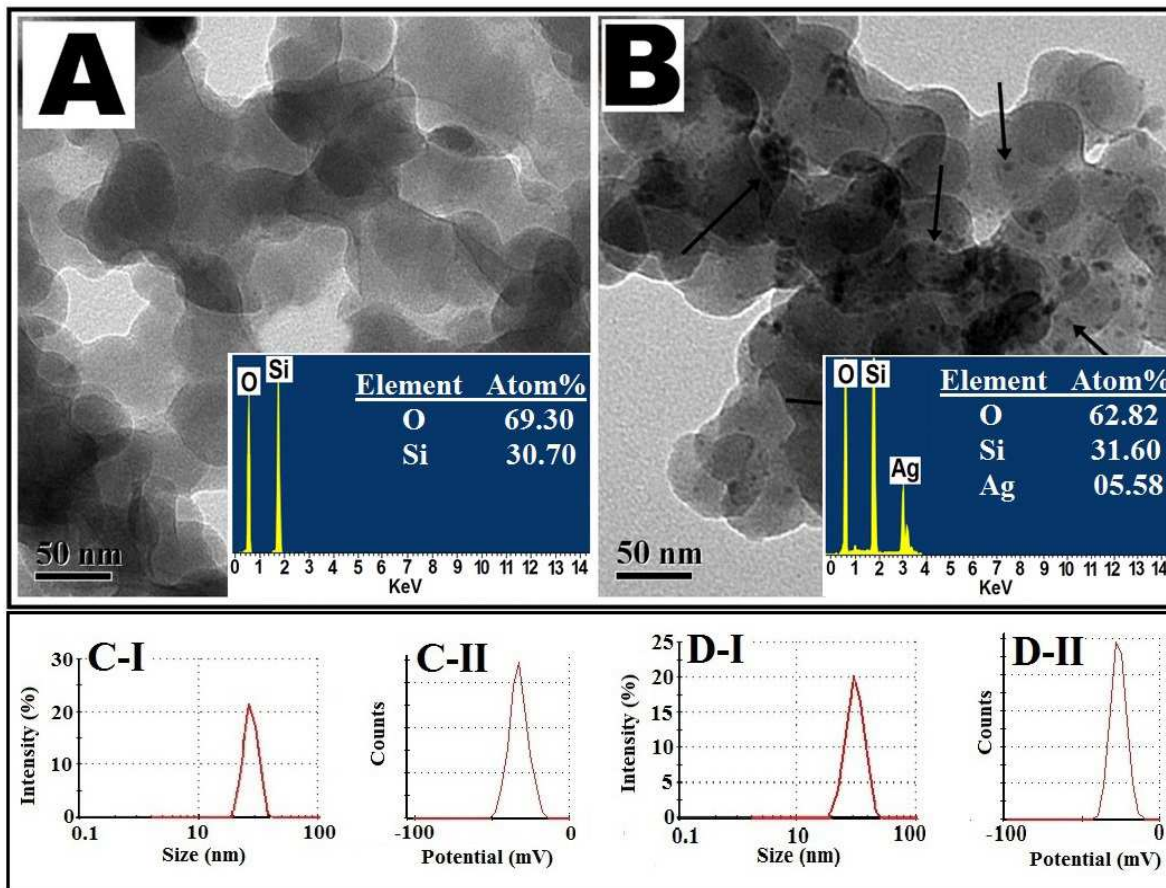


3

4    Figure 1: TEM image of (A) Silica NPs & (B) Silver-silica NPs with inset representing
5                elemental analysis by EDS. Zeta size (C-I & D-I) and Zeta potential (C-II & D-II)
6                distribution graph of silica NPs & silver-silica NPs respectively.
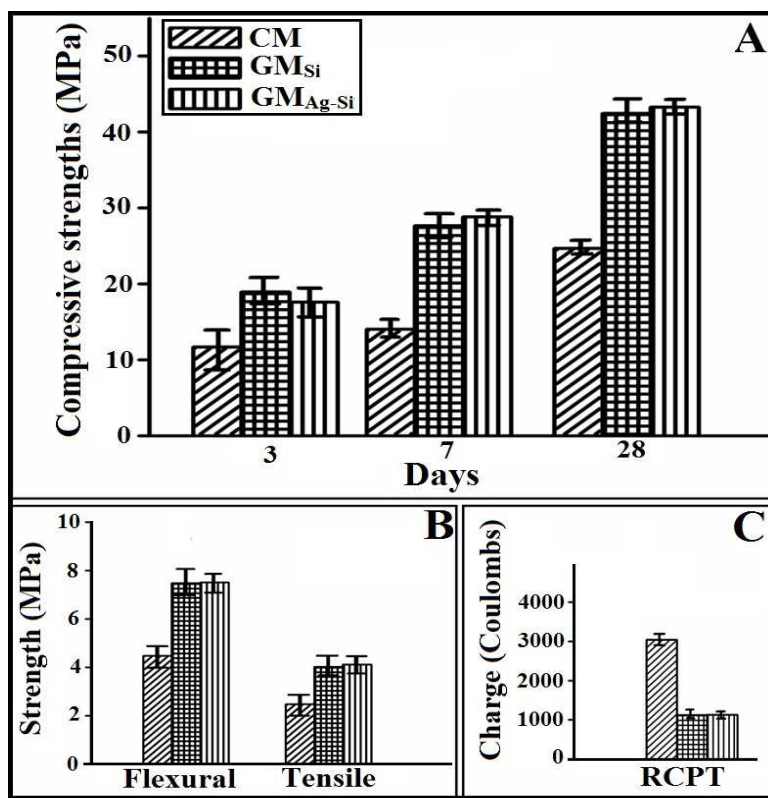
7

8

9

10
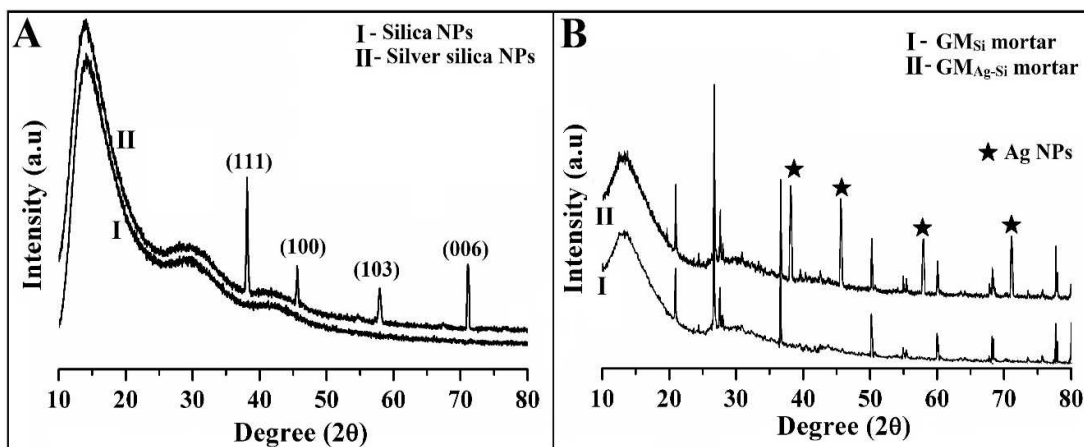
11

12　Figure 2A: XRD spectra of (I) $SiO_2$ NPs & (II) Ag-$SiO_2$ NPs.

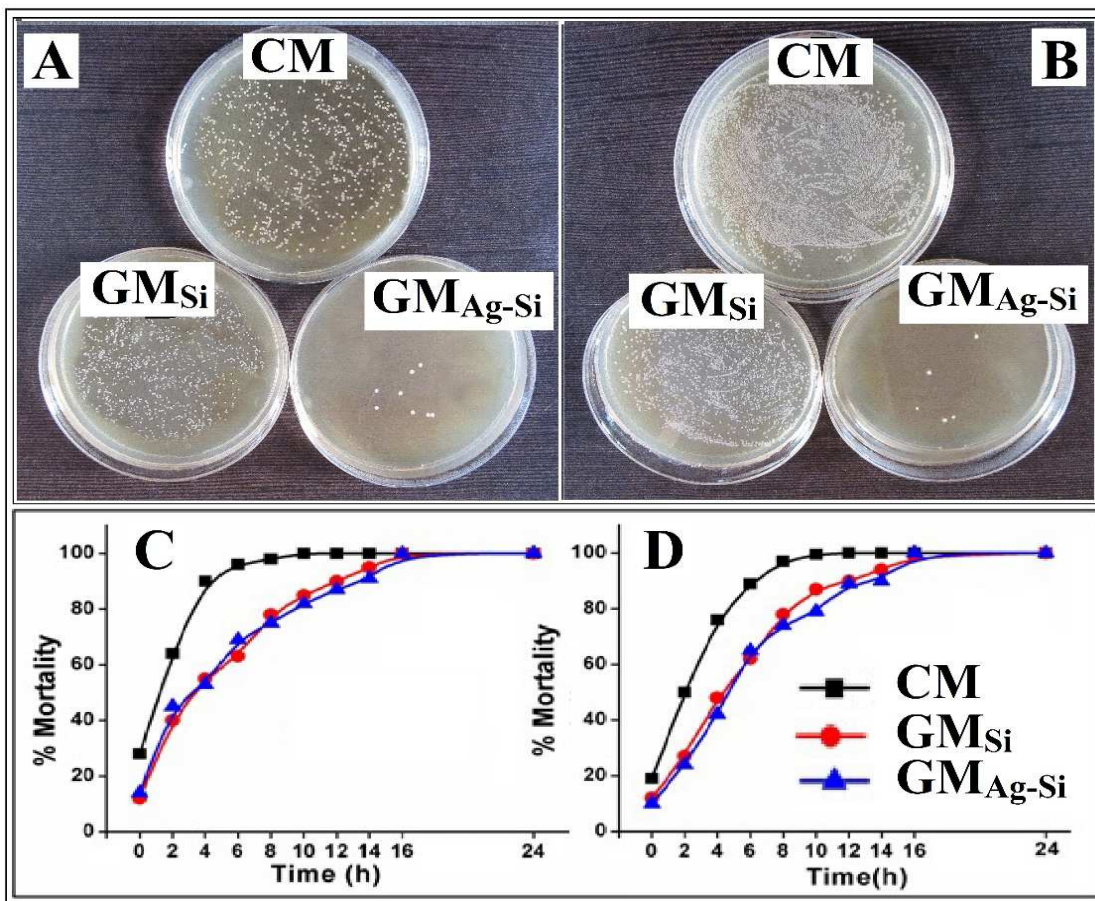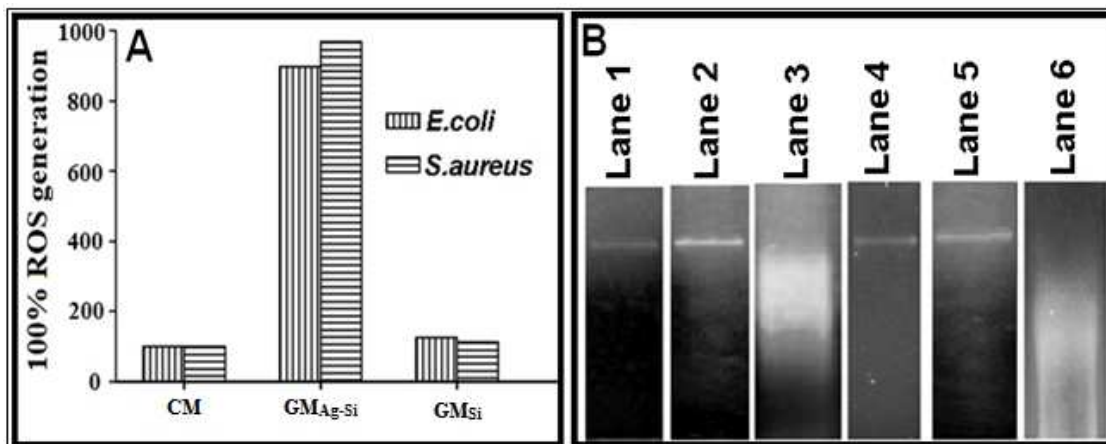13　Figure 2B: XRD spectra of (I) $GM_{Si}$ and (II) $GM_{Ag-Si}$.

14

15



16

17　Figure 3: (A) Compressive strengths (B) flexural & tensile strengths (C) RCPT of

18　　different mortar samples (CM, $GM_{Si}$ & $GM_{Ag-Si}$).

19

20

21

Figure 4: Photographs of colonies of (A) *E. coli* & (B) *S. aureus* incubated on agar plates obtained from cultivated suspensions with (CM, $GM_{Si}$ & $GM_{Ag-Si}$). Mortality curve of (C) Gram –ve bacteria (D) Gram +ve bacteria in presence of CM, $GM_{Si}$ & $GM_{Ag-Si}$.

Figure 5: ROS count of (A) different samples and (B) Gel electrophoresis images Lane-1: CM treated DNA (*E. coli*), Lane-2: GM$_{Si}$ treated DNA (*E. coli*), Lane-3: GM$_{Ag-Si}$ treated (*E. coli*), Lane-4: CM treated DNA (*S. aureus*), Lane-5: GM$_{Si}$ treated DNA (*S. aureus*), Lane-6: GM$_{Ag-Si}$ treated DNA (*S. aureus*).
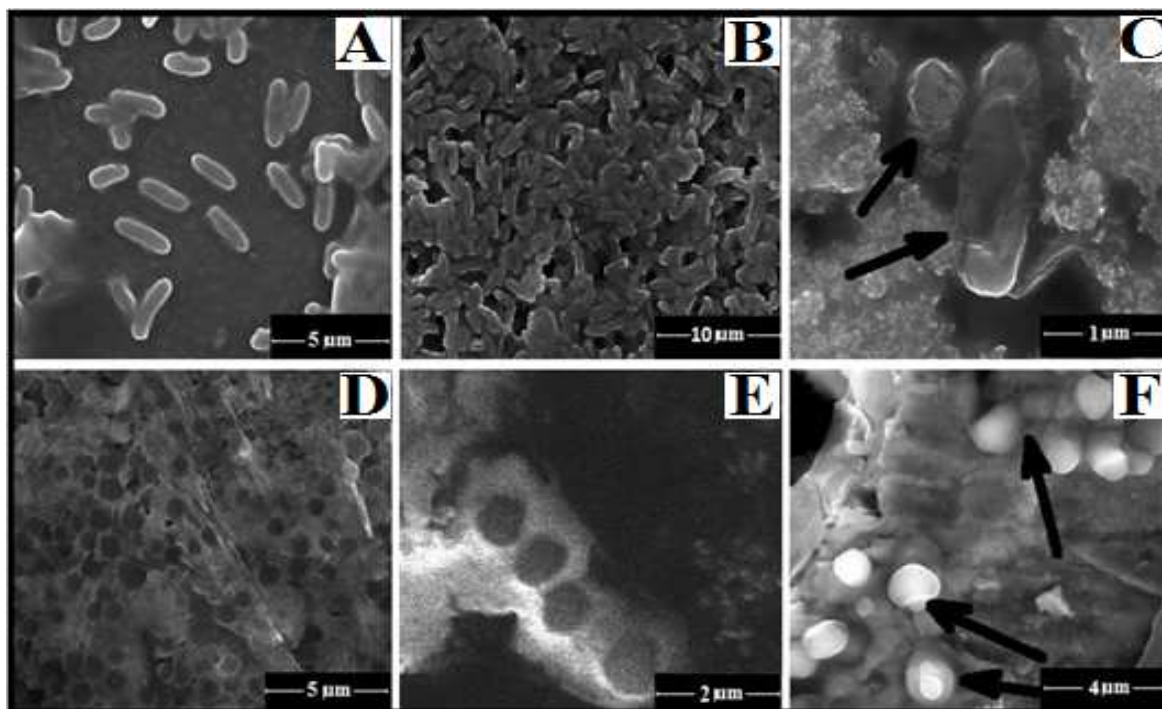


Figure 6: Fluorescence microscopic images of (A) CM treated *E. coli*, (B) GM$_{Si}$ treated *E. coli*, (C) GM$_{Ag-Si}$ treated *E. coli*, (D) CM treated *S. aureus*, (E) GM$_{Si}$ treated *S. aureus*, (F) GM$_{Ag-Si}$ treated *S. aureus* bacterial cells.

Figure 7:  FESEM images of (A) CM treated *E. coli*  (B) GM$_{Si}$ treated *E. coli*    (C) GM$_{Ag-Si}$ treated *E. coli* (D) CM treated  *S. aureus* (E) GM$_{Si}$ treated *S. aureus* (F) GM$_{Ag-Si}$ treated *S. aureus*.
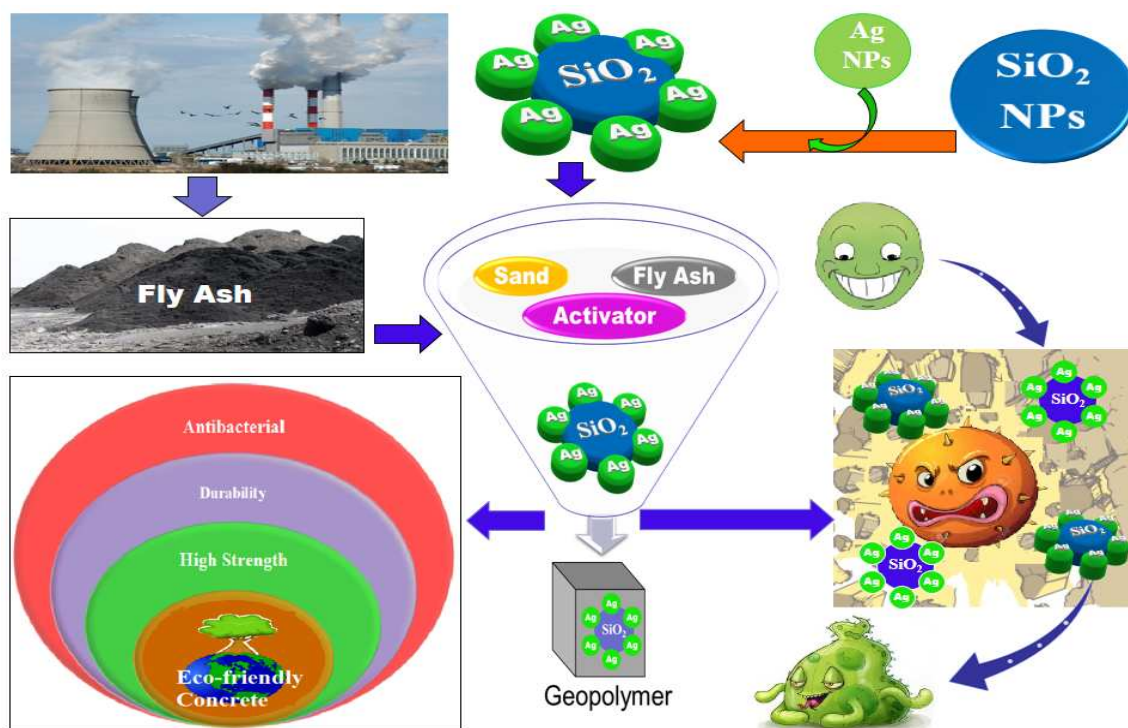
63    **Graphical Abstract:**



64

65    Schematic representation of anti-bacterial action of Silver-silica modified geopolymer mortar
66    for green construction technology.